Structure and properties of Bi 2 Ti 2 O 7 pyrochlore type phase stabilized by lithium

Jerome Lelievre, Pascal Marchet

Structure and properties of $Bi_2Ti_2O_7$ pyrochlore type phase stabilized by lithium

Jerome Lelievre, Pascal Marchet*

Université de Limoges SPCTS UMR 7315, Centre Européen de la Céramique, 12 Rue Atlantis, 87068 Limoges Cedex, France

* corresponding author:
Email address: pascal.marchet@unilim.fr

Abstract

A study of the Li_2O - Bi_2O_3 - TiO_2 ternary system evidenced a $Bi_2Ti_2O_7$ pyrochlore phase in a large range of composition, centered on $(Li_{1/2}Bi_{1/2})TiO_3$ (LBT). This composition led to a pyrochlore phase stable up to 1100°C, while pure $Bi_2Ti_2O_7$ phase has been reported as metastable, with decomposition temperature around 600°C. According to previous studies, this pyrochlore phase was not obtained without lithium and here only a few percent of lithium was necessary for stabilization. The structural study, performed by neutron diffraction, evidenced a cubic $Fd\bar{3}m$ structure (a = 10.317 Å), similar to the one of "pure" $Bi_2Ti_2O_7$ pyrochlore phase. The Li-ion is probably located on the Bi-site and is responsible for the stabilization of the pyrochlore structure. The electrical properties of the LBT composition were studied and appeared as very similar to the one of "pure" $Bi_2Ti_2O_7$. Because of its large thermal stability range, this pyrochlore phase appears to be a promising material for dielectric or tunability applications.

Keywords

Pyrochlore, solid state reaction, Li_2O-Bi_2O_3-TiO_2 phase-diagram, neutron diffraction, dielectric response, ionic conduction.

1. Introduction

$Bi_2Ti_2O_7$ is a pyrochlore compound whose existence as a stable compound is still controversial. To our knowledge, the first attempt to prepare this phase corresponds to the paper of Knop et al. in 1968 devoted to $A_2Ti_2O_7$ titanates. Their study of the $(Y_{1-x}Bi_x)_2Ti_2O_7$ solid solution evidenced a solid solution limit for x = 0.8 [1]. Therefore, the $Bi_2Ti_2O_7$ pyrochlore phase seems to not exist as a stable compound. Indeed, the Bi_2O_3 - TiO_2 phase diagram, first published by Speranskaya et al. [2], evidenced only $Bi_2Ti_4O_{11}$, $Bi_4Ti_3O_{12}$ and Bi_8TiO_{14}, this last compound being previously reported as $Bi_{12}TiO_{20}$ [3]. A later study of the liquidus by Bruton for the Bi_2O_3 rich range confirmed the existence of $Bi_{12}TiO_{20}$ instead of Bi_8TiO_{14} [4]. Then Kahlenberg et al. confirmed, for the central region of the phase diagram, that the only stable phases up to 1050°C are $Bi_2Ti_4O_{11}$ and $Bi_4Ti_3O_{12}$ [5]. Above 1100°C, a third minority pyrochlore phase appeared

together with the last compounds, as the result of a prolonged annealing, associated to bismuth losses. The lattice parameter of this pyrochlore phase is 10.3542 Å, in very good agreement with the value predicted by Knop et al. [1]. The structural study confirmed that this compound presents a defect pyrochlore structure, with compositions $Bi_{1.833}Ti_2O_{6.75}$ [5]. They also evidenced that a $Bi_2Ti_2O_7$ compound having the ideal stoichiometric composition should not be stable, so that the pyrochlore type in the Bi_2O_3 - TiO_2 system can be realized only in the form of a defect structure. This result agrees well with the review paper of Subramanian et al. devoted to $A_2Ti_2O_7$ titanates [6]. Their study, based upon ionic radii, evidenced that $Bi_2Ti_2O_7$ compound falls out of the stability range of the pyrochlore structure.

However, a $Bi_2Ti_2O_7$-like phase is frequently observed as the first crystallizing compound during the elaboration of thin films of similar materials, like $Bi_4Ti_3O_{12}$, by low temperature process such as sol-gel, chemical solution deposition method, RF magnetron sputtering or metal-organic chemical vapor deposition (MOCVD) [7-12].

Therefore, different authors elaborated successfully $Bi_2Ti_2O_7$ films by different methods such as chemical solution deposition, metalorganic decomposition or aerosol assisted chemical vapor deposition [13-18]. Finally $Bi_{1.74}Ti_2O_{6.62}$ and $Bi_2Ti_2O_7$ pyrochlore powders were successfully obtained by such methods, allowing structural studies [19, 20]. More recently, the use of microwave rapid sintering method allowed obtaining pellets of $Bi_2Ti_2O_7$ and the study of its physical properties [21]. This study also confirmed the thermodynamically instable behavior of $Bi_2Ti_2O_7$, which decomposes between 480-650°C, depending of thermal history of the samples. Therefore, this compound appears clearly as a metastable compound and stabilization of this phase would be extremely interesting in view of its properties.

Furthermore, our laboratory is involved in the search of lead-free perovskite materials. Indeed, at the present time, lead-based perovskite compounds, such as $Pb(Zr_{1-x}Ti_x)O_3$ (PZT) and $Pb(Mg_{1/3}Nb_{2/3})O_3$-$PbTiO_3$ (PMN-PT) are the best family of ferroelectric - piezoelectric materials. Their properties make them suitable for the manufacture of electromechanical devices such as actuators, sensors and so on. However, based on European directives, there are restrictions on the use of lead, because of its toxicity, and lead-based piezoelectric materials are only tolerated for piezoelectric devices. Therefore, new lead-free materials are widely investigated and some papers report potential candidates for the replacement of lead-based compounds, such as alkali niobates ((Na, K, Li)NbO_3), barium titanate ($BaTiO_3$) or alkali bismuth titanates $(Na_{1/2}Bi_{1/2})TiO_3$ (NBT) and $(K_{1/2}Bi_{1/2})TiO_3$ (KBT) [22-26].

Reported in 1961 by Smolenskii et al, the alkali bismuth titanates NBT and KBT evidenced the possibility to replace Pb^{2+} ion by the pseudo-ions (Na^+/Bi^{3+}) or (K^+/Bi^{3+}) [27] in $PbTiO_3$ perovskite compound. However, in the literature, no one reported the use of other alkali-ions such as Li^+ or Rb^+. Therefore, we recently tried to synthesize the $(Li_{1/2}Bi_{1/2})TiO_3$ (LBT) and $(Rb_{1/2}Bi_{1/2})TiO_3$ (RBT)

compounds by solid state reaction. The aim of this attempt was to check for the possible formation of a perovskite compound.

The Goldsmith factor [28], based on the ionic radii given by Shannon and Prewitt [29], calculated for $(Li_{1/2}Bi_{1/2})TiO_3$ (LBT) and $(Rb_{1/2}Bi_{1/2})TiO_3$ (RBT) are respectively 0.73 and 1.04 which means they are respectively too small and probably too large to accept a perovskite structure. Nevertheless, this is only a geometrical factor and there are other parameters that can influence the formation of a perovskite phase. In the case of RBT, no perovskite compound was evidenced by X-Ray diffraction. The results remained the same, even when the powders were calcined several times, using the same temperature (800°C) or higher temperature (900°C - 1000°C). Logically, no perovskite compound was evidenced in the case of the LBT sample. But surprisingly, we obtained at 800°C a pyrochlore phase, similar to the $Bi_2Ti_2O_7$ compound.

As presented hereinbefore, this compound doesn't exist in the binary phase diagram Bi_2O_3 - TiO_2. $Bi_2Ti_2O_7$ is considered as a metastable compound and is reported to not exist at temperature higher than 650°C. In our case it is surprisingly stabilized at least for the synthesis temperature of 800°C. Moreover, this phase seems to have interesting properties, such as high permittivity and low leakage current [13-18].

As this pyrochlore is said to be a promising materials, it is worth continuing this study, notably to try to understand how this phase has been stabilized. As a consequence, the aim of this study is: (i) to check for the conditions of stabilization of this pyrochlore phase by lithium-ion in the Li_2O - Bi_2O_3 - TiO_2 ternary system, (ii) to perform structural study of this compound and (iii) to study the dielectric behavior of such materials.

2. Experimental

The raw materials Li_2CO_3 (Alfa Aesar, 99.998%), Bi_2O_3 (Interchim, 99.975%) and TiO_2 (Aldrich, 99.8%) were first dried at 150°C. They were then weighed in the stoichiometric proportions and carefully mixed in an agate mortar before calcination at 800°C for 20h in alumina crucible.

Before sintering, a mixture of plasticizer and binder (polyethylene glycol and polyvinyl alcohol) was added to the powder in order to obtain suitable green pellets. These pellets were then shaped by uniaxial pressing (250 MPa) of the powders in a 10 mm diameter matrix. The pellets were finally sintered at 1050°C for 2h. Before electrical measurements, the ceramic samples were electroded on both sides using platinum paint. Dielectric measurements were performed between room temperature and 700°C using an impedance analyzer (Agilent 4294A, 100Hz – 1MHz). Impedance measurement were also performed using impedance meter (Solartron SI 1260, 100 mV DC signal) between 100 mHz and 5 MHz in a computer controlled cell allowing measurements between room temperature and 1000°C. The impedance circles were fitted by using the Zlive program [30]. DC conductivity measurements were also performed in a two points configuration by using a current source (Keithley 2400) and a voltmeter (Keithley 2000).

X-Ray Diffraction was performed on the raw powders and on the pellets using a θ/2θ diffractometer fitted with a fast detector (Bruker D8, Cu $K_{\alpha 1}$, Linkeye detector). Structural study of one sample was also performed by Powder Neutron Diffraction at the 3T2 diffractometer of the Leon Brillouin laboratory (Saclay, France). The powder (10 – 12g) was placed in a vanadium can and diffraction data were collected for 2θ angles between 4.5 and 121° at 20°C during 8 hours, using a 1.2289 Å wavelength. Structural resolution was performed by Rietveld method using the Jana 2006 software [31]. The chemical composition of powders was determined by Inductively Coupled Plasma - Atomic Emission Spectroscopy (ICP-AES) after dissolution in HCl/HF acid solution in microwave reactor. The microstructure of the ceramic samples was studied by scanning electron microscopy (SEM, JEOL JSM IT300) fitted with Energy Dispersive X-ray analysis (EDX).

3. Formation and stability of the pyrochlore phase

As explained in the introduction, a pyrochlore compound was easily obtained by classical solid state synthesis for the $(Li_{1/2}Bi_{1/2})TiO_3$ (LBT) composition, using a synthesis temperature of 800°C for 20h (fig. 1.a). Minority amounts of $Bi_4Ti_3O_{12}$, $Li_4Ti_5O_{15}$ and Li_2TiO_3 secondary phases are also observed. However, the X-ray diffraction pattern suggests large similarities with the previously reported $Bi_2Ti_2O_7$ pyrochlore phase. This compound being metastable, with decomposition in the range 480-650°C, obtaining this compound at 800°C is quite surprising. Therefore we made three assumptions to explain this result: (i) $Bi_2Ti_2O_7$ is missing in the Bi_2O_3 - TiO_2 binary phase diagram, (ii) the $Bi_2Ti_2O_7$ like compound obtained in our case is simply a metastable compound, that will decompose at higher temperatures and (iii) the pyrochlore phase is stabilized by the insertion of lithium ion. In the following part, these different hypotheses have been checked.

3.1. $Bi_2Ti_2O_7$: a missing phase in the binary phase diagram?

In order to check for this hypothesis, we tried to synthesize the $Bi_2Ti_2O_7$ pyrochlore phase by calcination of stoichiometric amounts of Bi_2O_3 and TiO_2 at 800°C for 20h. As evidenced by the XRD pattern (Fig. 1.b), the only observed phases are $Bi_4Ti_3O_{12}$ and $Bi_2Ti_4O_{11}$. Both compounds correspond well to the stable phases of the equilibrium phase diagram surrounding the 1:2 Bi_2O_3 - TiO_2 composition [2]. This result confirms the absence of the $Bi_2Ti_2O_7$ pyrochlore at 800°C. Thus we can conclude that lithium has probably a role in the stabilization of the pyrochlore phase.

3.2. Stability of the pyrochlore phase above 800°C?

Then, we tried to calcine the powders corresponding to LBT composition at higher temperature than our first experiments. We retained 1100°C for 20h, in order to check for a decomposition of the pyrochlore phase. The obtained powder was studied by XRD (Fig. 1.a). The results demonstrate: (i) a

large amount of remaining pyrochlore phase and (ii) an evolution of the secondary phases previously identified toward only one phase, $Li_2Ti_3O_7$. Thus we can conclude that the obtained pyrochlore may not be just a metastable phase and probably exists as a stable compound of the Li_2O - Bi_2O_3 - TiO_2 ternary system.

3.3. Stabilization of the pyrochlore phase by lithium ion?

Finally, in order to check for the stabilization by lithium, a composition close to $Bi_2Ti_2O_7$, containing only a few percent of lithium, has been synthesized. The selected formula is 0.02 Li_2O - 0.31 Bi_2O_3 - 0.67 TiO_2. The raw powders were calcined at 800°C for 20h, like in our previous experiments. The XRD pattern (Fig. 2) is different from the one previously obtained for the LBT composition. However, we could identify: (i) a pyrochlore phase in a lower proportion and (ii) the $Bi_4Ti_3O_{12}$ compound. Thus the presence of lithium, even in small amount, has an important effect on the stability of the pyrochlore phase, notably its stabilization.

3.4. Stability zone of pyrochlore phase

In order to check for the influence of the lithium content on the stability and on the amount of pyrochlore phase, a study of the Li_2O - Bi_2O_3 - TiO_2 ternary system was performed at 800°C for 20h synthesis time, around the $(Li_{1/2}Bi_{1/2})TiO_3$ composition. The aim of this study was to determine the influence of the amount of lithium on the proportion of pyrochlore phase. Four diagonals of the ternary system were retained, by fixing the percentage of TiO_2 at 60, 67, 74 and 80 mol% respectively, while the lithium content was changed (Fig. 3). The studied lines correspond to the formulae $Li_{2x}Bi_{(0.8-2x)}Ti_{0.6}O_{2.4}$ (60% TiO_2), $Li_{2x}Bi_{(0.66-2x)}Ti_{0.67}O_{2.33}$ (67% TiO_2), $Li_{2x}Bi_{(0.52-2x)}Ti_{0.74}O_{2.26}$ (74% TiO_2) et $Li_{2x}Bi_{(0.4-2x)}Ti_{0.8}O_{2.2}$ (80% TiO_2).

The amount of the observed phases was calculated on the basis of the XRD patterns, by using the intensity of their most intense diffraction peaks. The following formula was used for a rough calculation of the observed phases:

$$\%_j = \left(\frac{I_j}{\sum_i I_i}\right) \quad (2)$$

Where I_j is the measured intensity for the main peak of the considered phase and I_i is the value for all the observed phases. The results are reported in Table 1.

As reported in the literature and according to our previous results, the pyrochlore phase is not formed when the composition lies on the binary Bi_2O_3 - TiO_2. Thus, the compositions with a ratio of TiO_2/Bi_2O_3 equal to 60/40, 67/33 and 80/20 only led to the formation of $Bi_4Ti_3O_{12}$ (B4T3) and $Bi_2Ti_4O_{11}$ (B2T4) phases. This is again an evidence of the impact of lithium ion on the stabilization of the structure.

Finally, the phase diagram has been divided into four parts:

- Part 1: It corresponds to amount of pyrochlore above 50%, but with a lot of secondary phases. Moreover, the amount of TiO_2 is important and some of it remains at the end of the calcination.
- Part 2: The amount of pyrochlore is the highest for this area. There are only a few secondary phases in low proportion.
- Part 3: There are only a few secondary phases for this zone. However the amount of pyrochlore phase is really low.
- Part 4: The pyrochlore phase is in low proportion for nearly all the composition. The Aurivillius phase $Bi_4Ti_3O_{12}$ is easily stabilized which could be explained by the fact that the proportion of TiO_2 on this diagonal is the same as in the $Bi_4Ti_3O_{12}$ compound.

The lattice parameter of the pyrochlore was calculated for these diagonals of the ternary system. The linear evolution of the lattice parameter evidences for a solid solution domain, at least for a large part of the composition range (fig. 4). Since we didn't check systematically for all the compositions in the ternary system, it's difficult to determine precisely the limits of this solid solution. However, for the composition range close to the binary Bi_2O_3 - TiO_2, this limit seems to correspond to x= 10% for 60% TiO_2 and x = 5% for 67% TiO_2. For the diagonals corresponding to 74 and 80% TiO_2, this upper bound is more difficult to estimate but seems to correspond nearly to x = 5%. This confirms again that the pyrochlore phase doesn't exist without lithium.

Finally, the proportion of B2T2 pyrochlore phase is the most important in the zone 2. As a consequence, we used the 67%TiO_2 - 16.5%Bi_2O_3 - 16.5%Li_2O composition, circled in Fig.5, for the rest of the study. Indeed, this composition was the one exhibiting the highest proportion of pyrochlore phase. It corresponds to the hypothetical compound $(Li_{1/2}Bi_{1/2})TiO_3$ (LBT) studied in our preliminary experiments.

4. Structural study by Powder Neutron Diffraction

The sample of $(Li_{1/2}Bi_{1/2})TiO_3$ composition used for the Powder Neutron Diffraction (PND) was synthesized with the experimental route described earlier. Since the lithium and bismuth chemical elements are known as being volatile, the obtained powder was studied by ICP-AES. The chemical composition was determined as 16.4 mol% Bi_2O_3, 14.6 mol% Li_2O and 69 mol% TiO_2. The LBT initial composition was 16.5 mol% Bi_2O_3, 16.5 mol% Li_2O and 67 mol% TiO_2. Thus this result shows that minor amounts of lithium and bismuth have been lost during synthesis of the powder. The structural refinements were performed by Rietveld method using the Jana2006 software. The secondary phases $Li_4Ti_5O_{12}$ [32] and Li_2TiO_3 [33] were added as secondary phases for the structural refinements.

4.1. Initial structural model: the ideal pyrochlore structure

The pyrochlore compounds have a general formula $A_2B_2O_7$, and can be written as $A_2B_2O_6O'$, with four cristallographically nonequivalent kinds of atoms [6]. At first glance, the $(Li_{1/2}Bi_{1/2})TiO_3$ studied composition doesn't correspond to the general formula of pyrochlore. But with doubling of this formula, it may be noted that the $(Li,Bi)Ti_2O_6$ obtained formula tends to be similar to the one of pyrochlores, especially for the one containing vacancies (□), like $(□,A)B_2O_6□'$ pyrochlores [6].

The space group of the ideal pyrochlore is $Fd\bar{3}m$ with eight molecules per unit cell [6]. The first refinement on the PND data was thus performed in the space group $Fd\bar{3}m$, using the general positions of the pyrochlore structure: Bi at (0,0,0), Ti at $(\frac{1}{2},\frac{1}{2},\frac{1}{2})$, O at $(\frac{1}{8},\frac{1}{8},z)$ and O' at $(\frac{1}{8},\frac{1}{8},\frac{1}{8})$. The lithium has not been inserted on this first step of our study. Isotropic displacement parameters were used for all the atoms. Moreover, the occupancies of Bi and O' have been refined, since the $Bi_2Ti_2O_7$ pyrochlore compound has also been previously reported as a non-stoichiometric compound, with formula such as $Bi_{1.74}Ti_2O_{6.62}$ [19].

Quite a good fit was obtained for this first refinement (Gof = 3.28; R_p = 4.00%; R_{wp} = 5.52%, a = 10.317 Å), even if the displacement parameters for Bi and O are too high: U_{iso} = 0.051 $Å^2$ and U_{iso} = 0.036 $Å^2$. The final chemical formula after this step was $Bi_{1.57}Ti_2O_6O'_{0.91}$, evidencing bismuth and oxygen O' deficiency. Based on this, we choose to try to add the lithium-ion on the Bi site. The result of this refinement was similar to the first one, with the same reliability parameters. The only difference is that the final formula was $Li_{0.35}Bi_{1.65}Ti_2O_7$ (Gof = 3.27; R_p = 3.99%; R_{wp} = 5.52%, a = 10.317 Å). This formula corresponds to 27.5 mol% Bi_2O_3, 5.8 mol% Li_2O and 66.7 mol% TiO_2, indicating lithium and titanium deficiency compared to initial composition and ICP-AES measurements. This can be easily explained by the occurrence of the secondary phases $Li_4Ti_5O_{12}$ and Li_2TiO_3, which contain missing part of lithium and titanium.

In order to check another possible position for the lithium-ion, we also tried to insert the lithium ion on the Ti-site or even on Bi and Ti sites simultaneously. But in each case, there was no convergence of the refinement. This result means that Li-ion probably occupies the Bi-site.

4.2. Final model using anisotropic parameters and static displacement

As in the publication of Hector and Wiggins [20], anisotropic displacement parameters were used in order to try to improve the goodness of fit that fell to 2.90. However, the displacement parameters U_{ii} remained high and even increased with the use of the anisotropy (U_{ii}(Bi) = 0.061 $Å^2$ and U_{ii}(O') = 0.047 $Å^2$). As a consequence, the possibility of a static displacement of the bismuth-ion to the 96g (x,y,z) or 96h (0,y,-y) positions was tested. However, in our case, the refinement was not successful in both cases. This is in concordance with the absence of the (442) peak on PND pattern. The bismuth ion remained then on the 16c initial position.

However, these parameters remained quite high for the oxygen O' Thus this one has also been considered as being displaced from the $(\frac{1}{8},\frac{1}{8},\frac{1}{8})$ position of the ideal structure. As for $Bi_2Ru_2O_7$ and γ-$Bi_2Sn_2O_7$, the 32e site (x,x,x) was used for the oxygen O'. This atomic position is characteristic of a displacement toward or away from the vertex of the tetrahedron [20]. This did not result in a high improvement of the reliability's parameters (Gof = 2.88, R_p = 3.55%, R_{wp} = 4.86%). Nevertheless, the isotropic displacement parameters of the oxygen-ion decreased to better values (U_{iso} = 0.007 $Å^2$). The final formula can be identified as $Li_{0.32}Bi_{1.68}Ti_2O_6O'_{0.88}$ at the end of the refinements, with a refined lattice parameter of 10.317 Å, lower than the value of 10.379 Å reported for $Bi_2Ti_2O_7$ [20]. The final profile fit is given in Fig. 5 and the atomic positions in Table 2.

This formula corresponds to 28.0 mol% Bi_2O_3, 5.3 mol% Li_2O and 66.7 mol% TiO_2. As noticed for intermediate calculations (see. 4.1) this result indicates lithium and titanium deficiency, according to the occurrence of $Li_4Ti_5O_{12}$ and Li_2TiO_3 secondary phases.

The final structure (Fig. 5) highlights the disorder on the Bi and O' site. The displacement parameters are quite good at the end of the refinement. Bismuth-ion is the one which exhibits the highest displacement parameters, but this is probably due to its $6s^2$ lone pair. The lithium ion is thought to be located in the bismuth lacuna, as these refinements gave the best results. Moreover, this could explain the decrease of the cell parameters compared to the one reported by Hector and Wiggin [20].

5. Electrical properties

Dielectric properties

The relative permittivity ε' and dielectric losses tan(δ) of the LBT ceramic sample are represented in fig. 6. At 100 kHz and room temperature, the relative permittivity is 85 which is lower than the values of 115 at 500kHz reported for bulk by Esquivel et al. [21] and 118 at 100 kHz reported by Wu et al. for thin films [13]. The dielectric losses (100 kHz, room temperature) are low, tan(δ) = 0.016, and thus of the same order of magnitude as the value reported by Esquivel et al. for bulk. A relaxation is also observed for a large range of temperatures. This has already been reported in the literature [21, 35-38] for other similar pyrochlore compounds, and for $Bi_2Ti_2O_7$ compound [21, 35-38]. This phenomenon can be enhanced here by the fact that two ions occupy one site, with Li and Bi on the 16c site.

Furthermore, the values of tan(δ) above 100°C are quite high, which can be a consequence of the relaxation. This can also point out that the pyrochlore we obtained presents ionic conductivity. For this reason, electrical conduction measurements were performed.

Conduction properties

Based on the impedance spectroscopy data, measured from 100 mHz to 5MHz in the temperature range 20°C – 600°C, the Nyquist diagrams were represented. The results were studied only above 150°C, since lower temperatures gave no impedance circle. A high frequency phenomenon, associated to the inductance of the wires is visible for all curves. The corresponding points have not been used for the data treatment. These diagrams have then been studied using the Zlive software [30]. The used model is based on the serialization of R//CPE (Constant Phase Element) cells.

Two models have been used to refine the diagrams. The first one exhibited two inputs at high frequency (150°C to 475°C), whereas the second (500°C to 600°C) used only one (fig. 7). The resistance values were extracted, in order to plot their evolution with temperature and to determine the activation energies, based on the Arrhenius law: $\sigma = \sigma_0 \times \exp(-\frac{E_a}{kT})$ or $\ln(\sigma) = \ln(\sigma_0) - \frac{E_a}{kT}$. A linear model, $\ln(\sigma) = (A / T) + B$, was used for calculation of the activation energy (fig. 8). The reliability and the equation of the linear law used to refine the plots are given in Table 3.

Electrical resistance was also measured using a DC device. The same two thermal ranges were also evidenced, but the calculated activation energies were lower, probably because of the effects of relaxation behavior on the results for AC measurements (fig. 8). For the low temperature range (150 - 475°C), the calculated activation energy is 0.37 eV while for the high temperature range, the value is 0.67 eV.

The two contributions obtained for the range 150°C - 475°C can't be separated for DC measurements. Indeed, they differ only because of frequency effects. However they exhibit relatively the same activation energy for AC measurements. This result could have different sources: (i) the pyrochlore was present with two distinct grain size, (ii) there is a contribution of the grain boundaries or (iii) there are grains which exhibited the same phenomenon but with different composition.

The observation of the pellets by Scanning Electron Microscopy (fig. 9) revealed that the secondary phases are located in some crystallized area and not at the grain boundaries. Furthermore, a study of the chemical composition of the grains was performed. The EDS study (fig. 9) revealed that these domains have different composition, as there is no bismuth in the dark zones. However, it was not possible by this method to investigate the presence of lithium, non-detectable by EDS. However, the $Li_4Ti_5O_{12}$ secondary phase evidenced by X-ray diffraction can be identified here as the regions where bismuth is missing (white circles in fig. 9). The grain size of the secondary phase is around 2 to 3 µm, while the one of pyrochlore phase is larger and between 2 and 10µm. This seems to indicate that the two phenomena and the associated activation energies observed for the low temperature range (150 - 475°C°) corresponds to both phases. The obtained value of the activation energies (0.37 - 0.67 eV) corresponds quite well to the one reported for Bi-based pyrochlore compounds (0.36 - 0.60 eV) [39].

6. Discussion

$Bi_2Ti_2O_7$ is a pyrochlore compound whose existence was controversial for a long time. Indeed, only recent papers succeeded in the preparation of "pure" pyrochlore phases $Bi_{1.74}Ti_2O_{6.62}$ or $Bi_2Ti_2O_7$ [19-21]. Esquivel-Elizondo et al. [21] clearly demonstrated that, due to the difficulty in preparing a single phase of the pyrochlore structure, properties have been incorrectly ascribed to this compound. Misleading results were frequently obtained, like ferroelectricity, because of the occurrence of secondary phases like $Bi_4Ti_3O_{12}$ or $Bi_2Ti_4O_{11}$ which are ferroelectric compounds. However, the recent results confirmed that "pure" $Bi_2Ti_2O_7$ pyrochlore phase can only be obtained with chemical synthesis. It's only by using a very fast sintering method that Esquivel-Elizondo et al. succeeded in obtaining sintered sample without decomposition and secondary phases.

However, our results agrees well with the one of Subramanian et al which established a stability range for $(A^{3+})_2(B^{4+})_2O_7$ pyrochlore compounds [6]. This one is based upon the relative ionic radii (RR) of A^{3+} and B^{4+} ions: RR = [r(A^{3+}) / r(B^{4+})]. The ionic radius of Bi^{3+} is 1.17 Å (Coordination Number VIII) while the one of Ti^{4+} (Coordination Number VI) is 0.605 Å [29]. Therefore, RR = 1.933 for $Bi_2Ti_2O_7$, thus outside of the stability range of this pyrochlore family (RR = 1.46 to 1.80) [6]. As a consequence, the replacement of half Bi^{3+} by Li^+, whose ionic radius is 0.92 Å (Coordination Number VIII), induce a mean ionic radius of 1.045 Å for the (Li^+, Bi^{3+}) pseudo-ion in the A-site of the $A_2B_2O_7$ formula. As a consequence, the RR mean value decrease up to 1.72, in the stability range of the $(A^{3+})_2(B^{4+})_2O_7$ pyrochlore phases. This implies that the mixed occupancy of the A-site induce the stabilization of the pyrochlore structure, as observed here before where we obtained a stabilization of the $(Li_{1/2}Bi_{1/2})TiO_3$ / $(Li,Bi)Ti_2O_6$ composition.

The structural refinement of this composition evidenced that Li-ion is effectively located in the Bi-site, leading to the formula $Li_{0.32}Bi_{1.68}Ti_2O_6O'_{0.88}$. Some differences with the results of Hector et al. are also observed. Hector introduced a displacement of the Bi ion from their ideal (0,0,0) position (16c), toward (0, y, $\bar{y}$) position (96g). He also introduced a splitting of the O' positions, into a mixed site occupancy of $(\frac{1}{8},\frac{1}{8},\frac{1}{8})$ (8a) and (x, x, x) (32e) positions. These displacements were necessary in order to take account of the static displacement of the Bi-ion, due to the active lone pair, and the structural disorder of oxygen ions.

In our case: (i) the Bi remains in the ideal (0,0,0) position (16c) of ideal pyrochlore structure, (ii) only one crystallographic site is needed for the O' position, which is not the $(\frac{1}{8},\frac{1}{8},\frac{1}{8})$ (8a) position of ideal pyrochlore structure. The (x, x, x) (32e) crystallographic site used for the O' ion corresponds to a splitting into four equivalent positions around the ideal one, each of these sites being occupied by ¼ of the oxygen ions. Logically, this splitting indicates disorder of the oxygen-ions around the (Li^+, Bi^{3+}) pseudo-ion.

The coordination cation polyhedrons are represented fig. 10. As for ideal pyrochlore structure [6], the Ti-ion is located in a trigonal antiprism, with six oxygen ions at 1.959 Å. This distance is quite similar to the 1.965 Å value of "pure" $Bi_2Ti_2O_7$ [20]. The measured angles, in the equatorial plane of this distorted octahedra, are 92.626° and 87.375, close the values of 92.48° and 87.52° for $Bi_2Ti_2O_7$ [20]. The Ti-O-Ti angles are 137.3°, again close to the 137.51° of $Bi_2Ti_2O_7$.

As for the ideal structure of $A_2B_2O_6O'$ formula, the coordination polyhedron of Bi-ion correspond to a scalenohedron, with six "O" ions at equal distance from the central cation and two O' ions at larger distance [6]. Here, six oxygen-ions in 48f position, i.e. the "O" ions of the $A_2B_2O_6O'$ formula, are located at 2.611 Å of the (Li^+, Bi^{3+}) pseudo-ion. The "O'" ion, in 32e position, is located in a tetrahedron, around the 8a "normal" position of the ideal pyrochlore structure. Thus different Bi-O associated distances are encountered: 2.362 Å (3 bonds) and 1.913 Å (1 bond). In addition, the (Li^+, Bi^{3+}) pseudo-ion is represented by a "flat" ellipsoid, associated to the positional disorder induced both by the mixed occupancy of this crystallographic site and the $6s^2$ active lone-pair of Bi-ion. The Bi-O-Ti angles are 105.09°, similar to the 104.46° of "pure" $Bi_2Ti_2O_7$. Thus the structure appears to be very similar to the one of $Bi_2Ti_2O_7$.

Bond valence calculation was also performed using the values of Brown et al. [40]. The bond valence sum (BVS) for Ti^{4+} is 4.06 ± 0.4, in agreement with the value expected for this ion. BVS for Bi resulted in 2.84 ± 0.5, whereas Hector et al. calculated a value of 3.01 for "pure" $Bi_2Ti_2O_7$ and 2.73 for ideal pyrochlore structure without bismuth or oxygen displacements. This value indicates that our result is intermediate between the two structures, probably because of the presence of lithium. The calculated BVS for Li^+ is 0.52 ± 0.1, in agreement with our difficulty to localize precisely the lithium and to determine the exact content of this ion in the structure.

7. Conclusion

A study of the Li_2O - Bi_2O_3 - TiO_2 ternary system was performed at 800°C in order to determine the compositional stability range of $Bi_2Ti_2O_7$ phase. This study demonstrated for a large solid-solution domain, centered on the $(Li_{1/2}Bi_{1/2})TiO_3$ composition. The pyrochlore phase obtained for this formula was evidenced as stable up to 1100°C. The structure of the pyrochlore phase corresponding to this composition has been studied by neutron diffraction. The results evidenced that the obtained structure is very similar to the one of "pure" $Bi_2Ti_2O_7$ pyrochlore phase. The structures is cubic with $Fd\bar{3}m$ space group and a lattice parameter of 10.317 Å, close to the value of 10.379 Å reported for $Bi_2Ti_2O_7$.

The chemical formula determined by the Rietveld refinement is $Li_{0.32}Bi_{1.68}Ti_2O_6O'_{0.88}$. The structural study demonstrated that the Li-ion is probably located on the Bi-site and thus responsible for the stabilization of the pyrochlore structure.

The ionic conductivity of this material was studied, since lithium ion could contribute to this phenomenon together with oxygen ions. The activation energy of conducting phenomena was determined as being around 0.62 to 0.96 eV, with two different ranges. A relaxor behavior is observed in dielectric properties on a large range of temperatures, like for "pure" $Bi_2Ti_2O_7$ and other Bi-based pyrochlore phases. Because of its large thermal stability range, this $Bi_2Ti_2O_7$ pyrochlore type phase appears thus as a promising materials for dielectric or tunability applications, like for other similar Bi-based pyrochlore compounds.

Acknowledgment

J. Lelièvre gratefully acknowledge the "Conseil Regional du Limousin" for the Ph-d grant which allowed this work.

References

[1] O. Knop, F. Brisse, L. Castelliz, Pyrochlores. V. Thermoanalytic, X-ray, neutron, infrared, and dielectric studies of $A_2Ti_2O_7$ titanates, Can. J. Chem. 47 (1969) 971-990

[2] E. I. Speranskaya, I. S. Rez, L. V. Kozlova, V. M. Skorikov, V. I. Slavov, Bismuth oxide–titanium dioxide system, Izv. Akad. Nauk SSSR, Neorg. Mater. 1 (1965), 232-235; Inorg. Mater. (Engl. Transl.) 1 (1965) 213-216.

[3] E. M. Levin and R. S. Roth, Polymorphism of bismuth sesquioxide. II. Effect of oxide additions on the polymorphism of Bi_2O_3, J. Res. Natl. Bur. Stand. A68 (1964)197-206.

[4] T.M. Bruton, Study of the liquidus in the system Bi_2O_3,-TiO_2 J. Solid State Chem. 9 (1974) 173-175

[5] V. Kahlenberg, H. Bohm, On the existence of a Pyrochlore-type phase in the system Bi_2O_3 - TiO_2, Cryst. Res. Technol. 30 (1995) 237-241

[6] M.A. Subramanian, G. Aravamudan, G.V. Subba Rao, Oxide pyrochlores – a review, Prog. Solid St. Chem. 15 (1983) 55-143

[7] Y. Lu, D.T. Hoelzer, W.A. Schulze, B. Tuttle, B.G. Potter, Grain-oriented ferroelectric bismuth titanate thin film prepared from acetate precursor, Mater. Sci. Eng. B39 (1996) 41-47

[8] K.S. Hwang, Effect of substrates on epitaxy of $Bi_4Ti_3O_{12}$ thin films by dipping-pyrolysis process, Mater. Chem. Phys. 65 (1998) 222-225

[9] M. Yamaguchi, T. Nagatomo, Preparation and properties of $Bi_4Ti_3O_{12}$ thin films grown at low substrate temperatures, Thin Solid Films 348 (1999) 294-298

[10] S. Sun, P. Lu, P.A. Fuierer, Oriented bismuth titanate thin films by single-solid-source metal-organic chemical vapour deposition, J. Cryst. Growth 205 (1999) 177-184

[11] L.B. Kong, J. Ma, Randomly oriented $Bi_4Ti_3O_{12}$ thin films derived from a hybrid sol-gel process, Thin Solid Films 379 (2000) 89-93

[12]K.S. Hwang, C.K. Kim, S.B. Kim, J.T. Kwon, J.S. Lee, Y.H. Yun, Y.H. Kim, B.A. Kang, Preparation of epitaxial and polycrystalline bismuth titanate thin films on single crystal (100) MgO by chemical solution deposition, Surf. Coat. Technol. 150 (2002) 177-181

[13] X. Wu, S. W. Wang, H. Wang, Z. Wang, S. X. Shang, et M. Wang, Preparation and characterization of $Bi_2Ti_2O_7$ thin films by chemical solution deposition technique, Thin Solid Films 370 (2000) 30-32

[14] S. W. Wang, H. Wang, X. Wu, S. Shang, M. Wang, Z. Li, W. Lu, Rapid thermal processing of $Bi_2Ti_2O_7$ thin films grown by chemical solution decomposition, J. Cryst. Growth 224 (2001) 323–326

[15] Y. Hou, M. Wang, X.-H. Xu, D. Wang, H. Wang, S.-X. Shang, Dielectric and ferroelectric properties of nanocrystalline $Bi_2Ti_2O_7$ prepared by a metallorganic decomposition method, J. Am. Ceram. Soc. 85 (2002)3087–3089

[16] S. W. Wang, W. Lu, N. Li, H. Wang, M. Wang, X.C. Shen , Insulating properties of rapid thermally processed $Bi_2Ti_2O_7$ thin films by a chemical solution decomposition technique, Mater. Res. Bull. 37 (2002) 1691-1697

[17] Y. Hou, T. Lin, Z. Huang, G. Wang, Z. Hu, J. Chu, X. Xu, M. Wang, Electrical and optical properties of $Bi_2Ti_2O_7$ thin films prepared by metalorganic decomposition method, Appl. Phys. Lett. 85 (2004) 1214-1216

[18] A. McInnes, J. S. Sagu, et K. G. U. Wijayantha, Fabrication and photoelectrochemical studies of $Bi_2Ti_2O_7$ pyrochlore thin films by aerosol assisted chemical vapour deposition, Mater. Lett. 137 (2014) 214-217

[19] I. Radosavljevic, J. S. O. Evans, et A. W. Sleight, Synthesis and structure of pyrochlore-type bismuth titanate, J. Solid State Chem. 136 (1998) 63-66

[20] A. L. Hector et S. B. Wiggin, Synthesis and structural study of stoichiometric $Bi_2Ti_2O_7$ pyrochlore, J. Solid State Chem. 177 (2004) 139-145

[21] J. R. Esquivel-Elizondo, B. B. Hinojosa, J. C. Nino, $Bi_2Ti_2O_7$: It is not what you have read, Chem. Mater. 23 (2011) 4965-4974

[22] M. D. Maeder, D. Damjanovic, and N. Setter, Lead free piezoelectric materials, J. Electroceramics 13 (2004) 385–392

[23] Y. Saito, H. Takao, T. Tani, T. Nonoyama, K. Takatori, T. Homma, T. Nagaya, M. Nakamura, Lead-free piezoceramics, Nature 432 (2004) 84–87

[24] S. Zhang, R. Xia, and T. R. Shrout, Lead-free piezoelectric ceramics vs. PZT?, J. Electroceramics, 19 (2007) 251–257

[25] T. Takenaka, H. Nagata, Y. Hiruma, Y. Yoshii, and K. Matumoto, Lead-free piezoelectric ceramics based on perovskite structures, J. Electroceramics 19 (2007) 259–265

[26] W. Li, Z. Xu, R. Chu, P. Fu, and G. Zang, Piezoelectric and dielectric properties of $(Ba_{1-x}Ca_x)(Ti_{0.95}Zr_{0.05})O_3$ lead-free ceramics, J. Am. Ceram. Soc. 93 (2010) 2942–2944

[27] G. A. Smolenskii, V. A. Isupov, A. I. Agranovskaya, and N. N. Krainik, New ferroelectrics of complex composition. 4., Sov. Phys.-Solid State 2 [11] (1961) 2651–2654

[28] G. Beskow, V. M. Goldschmidt: Geochemische Verteilungsgesetze der Elemente, Geol. Foereningan Stockh. Foerhandlingar 46 [6–7] (1924) 738–743

[29] R. D. Shannon, Revised effective ionic radii and systematic studies of interatomic distances in halides and chalcogenides, Acta Crystallogr. A32 (1976) 751–767

[30] Zlive: Samuel Georges, ZLive, Le Mans, 2003.

[31] V. Petricek, M. Dusek, and L. Palatinus, Crystallographic Computing System JANA2006: General features, Z. Für Krist. - Cryst. Mater. 229 (2014) 345-352

[32] Y.-J. Gu, Z. Guo, and H.-Q. Liu, Structure and electrochemical properties of $Li_4Ti_5O_{12}$ with Li excess as an anode electrode material for Li-ion batteries, Electrochimica Acta 123 (2014) 576–581

[33] K. Kataoka, Y. Takahashi, N. Kijima, H. Nagai, J. Akimoto, Y. Idemoto, K. Ohshima, Crystal growth and structure refinement of monoclinic Li_2TiO_3, Mater. Res. Bull. 44 (2009) 168–172

[34] E. Aleshin, R. Roy, Crystal chemistry of Pyrochlore, J. Am. Ceram. Soc. 45 (1962) 18-25

[35] J. C. Nino, M. T. Lanagan, and C. A. Randall, Dielectric relaxation in Bi_2O_3–ZnO–Nb_2O_5 cubic pyrochlore, J. Appl. Phys. 89 (2001) 4512–4516

[36] T. A. Vanderah, M.W. Lufaso, A.U. Adler, I. Levin, J.C. Nino, V. Provenzano, P.K. Schenck, Subsolidus phase equilibria and properties in the system Bi_2O_3:$Mn_2O_{3\pm x}$:Nb_2O_5, J. Solid State Chem. 179 (2006) 3467–3477

[37] R. S. Roth, T.A.Vanderah, P. Bordet, I.E. Grey, W.G. Mumme, L. Cai, J.C. Nino, Pyrochlore formation, phase relations, and properties in the CaO–TiO_2–$(Nb,Ta)_2O_5$ systems, J. Solid State Chem. 181 (2008) 406–414

[38] C. G. Turner, J. R. Esquivel-Elizondo, and J. C. Nino, Dielectric properties and relaxation of $Bi_2Ti_2O_7$, J. Am. Ceram. Soc. 97 (2014) 1763–1768

[39] H. Du, X. Yao, H. Wang, Dielectric properties of pyrochlore $(Bi_{1.5}Zn_{0.5})(Nb_{0.5}M_{1.5})O_7$ (M = Ti, Sn, Zr and Ce) dielectrics, Appl. Phys. Lett. 88 (2006) 212901

[40] I.D. Brown, D. Altermatt, Bond-valence parameters obtained from a systematic analysis of the inorganic crystal structure database, Acta Crystallogr. B41 (1985) 244-247

Tables

Table 1 : List of the phases formed in this study

(B2T2 = $Bi_2Ti_2O_7$; B4T3 = $Bi_4Ti_3O_{12}$; B2T4 = $Bi_2Ti_4O_{11}$; L4T5 = $Li_4Ti_5O_{12}$; L2T = Li_2TiO_3)

Initial composition		Final composition					
$\%TiO_2$	$\%Li_2O$	%B2T2	%B4T3	%B2T4	%L4T5	%TiO2	%L2T
60	0	0	100	0	0	0	0
	5	5	94.3	0	0	0	0.7
	10	14.6	84	0	0	0	1.4
	15	21.2	76.2	0	0	0	2.5
	25	56.7	33.8	0	0	0	9.6
	35	42.5	27.6	0.2	4.2	0	25.4
67	0	0	83.7	16.3	0	0	0
	2	35	65	0	0	0	0
	4	42.5	57.5	0	0	0	0
	5	59.8	40.2	0	0	0	0
	10	68.5	29.3	0	0.5	0	1.7
	16.5	92.1	4.2	0	1.3	0	2.4
	25	86.4	0	0	6.9	0	6.7
74	5	70.8	5.4	20.3	0.5	3.1	0
	10	78.9	3.4	10.1	1.9	5	0.7
	15	75.5	0.4	10	4.4	8.8	1
	20	62	3.9	12	11.4	10.6	3.2
80	0	0	34.9	65.1	0	0	0
	5	53.1	0	33.9	1.1	11.7	0.3
	10	55.9	0	23.8	3.1	16.9	0.3
	15	50.2	0	7.2	8.7	32.9	0.9

Table 2 : Refined cristallographic parameters of the pyrochlore $Li_{0.38}Bi_{1.62}Ti_2O_6O'_{0.89}$ in the $Fd\bar{3}m$ space group

	Site	Oc.	x	y	z	U_{11}, U_{22}, U_{33}	U_{12}, U_{13}, U_{23}
Bi	16c	0.069	0	0	0	0.061	-0.028
Li	16c	0.014	0	0	0	0.061	-0.028
Ti	16d	0.083	0.5	0.5	0.5	0.005	0
O	48f	0.250	0.125	0.125	0.430	0.007	0
O'	32e	0.037	0.107	0.107	0.107	0.007	0
Gof			2.88	R_p	3.55%	R_{wp}	4.86%

Table 3 : Results of the Arrhenius law refinement for conductivity phenomena in the LBT ceramic sample

		a	b	R^2	Ea (eV)
150°C-475°C	HF	-7209.6	-0.425	0.999	0.621
	MF	-7638.2	-0.015	0.999	0.658
500°C-600°C	HF	-11160.3	4.168	0.999	0.962

Figure Caption

Fig. 1: (a) XRD pattern of the $(Li_{1/2}Bi_{1/2})TiO_3$ (LBT) powder calcined at 800°C for 20h, 1100°C for 20h and calculated $Bi_2Ti_2O_7$ pattern obtained from Esquivel et al [21], (b) XRD pattern of the stoichiometric composition corresponding to $Bi_2Ti_2O_7$ calcined at 800°C for 20h (color online)

Fig. 2 : XRD pattern for the 0.02 Li_2O - 0.31 Bi_2O_3 - 0.67 TiO_2 powder calcined at 800°C for 20h (color online)

Fig. 3: Phase diagram of the ternary system TiO_2 -Bi_2O_3 - Li_2O (compositions in mol %) indicating the calcined compositions (color online)

Fig. 4: Evolution of the lattice parameter of the pyrochlore phase along four diagonals of the phase diagram (color online)

Fig. 5: (a) Final profile for the refinement of the LBT compound and (b) Representation of the pyrochlore $Li_{0.38}Bi_{1.62}Ti_2O_6O'_{0.89}$ structure in the $Fd\bar{3}m$ space group (color online)

Fig. 6: (a) Relative permittivity ε' and (b) dielectric losses for the LBT ceramic sample (color online)

Fig. 7: Examples of two refined Nyquist diagrams: (a) at 325°C (low temperature range and (b) 550°C (high temperature range) (color online)

Fig. 8: Arrhenius plot of the data obtained for LBT ceramic sample from (a) DC measurements and (b) the AC impedance circles (color online)

Fig. 9: (a) SEM observation of the LBT pellet and EDX study of the pellet for (b) Ti, (c) Bi and (d) oxygen (color online)

Fig. 10: cation coordination spheres with selected bond lengths and angles for (a) titanium) and (b) bismuth (color online)

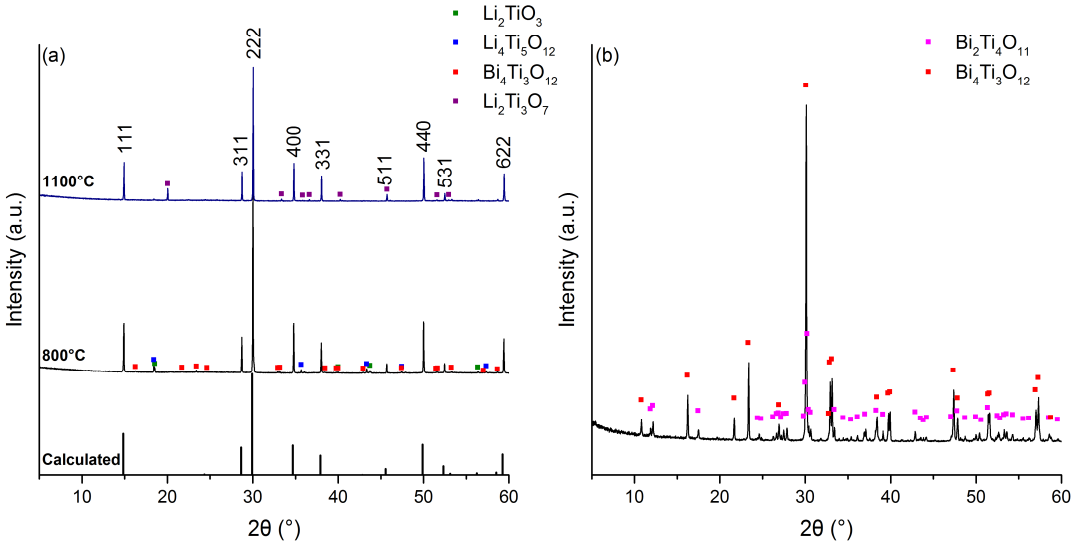

Fig. 1: (a) XRD pattern of the $(Li_{1/2}Bi_{1/2})TiO_3$ (LBT) powder calcined at 800°C for 20h, 1100°C for 20h and calculated $Bi_2Ti_2O_7$ pattern obtained from Esquivel et al [21], (b) XRD pattern of the stoichiometric composition corresponding to $Bi_2Ti_2O_7$ calcined at 800°C for 20h (color online)

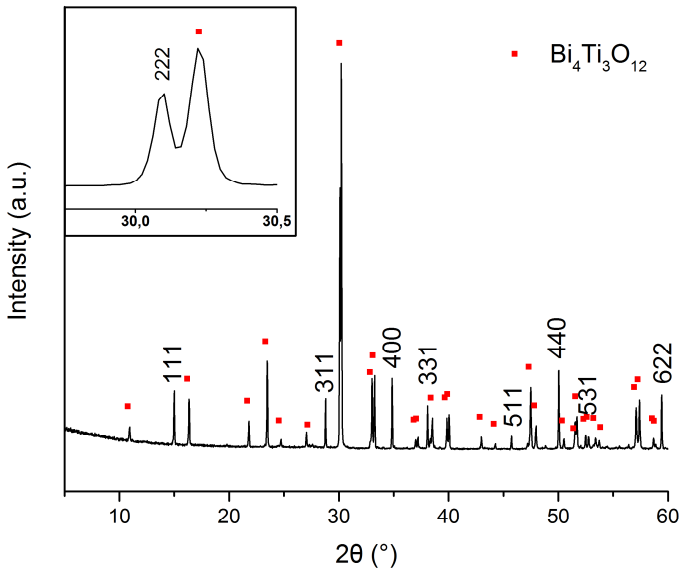

Fig. 2 : XRD pattern for the 0.02 Li_2O - 0.31 Bi_2O_3 - 0.67 TiO_2 powder calcined at 800°C for 20h (color online)

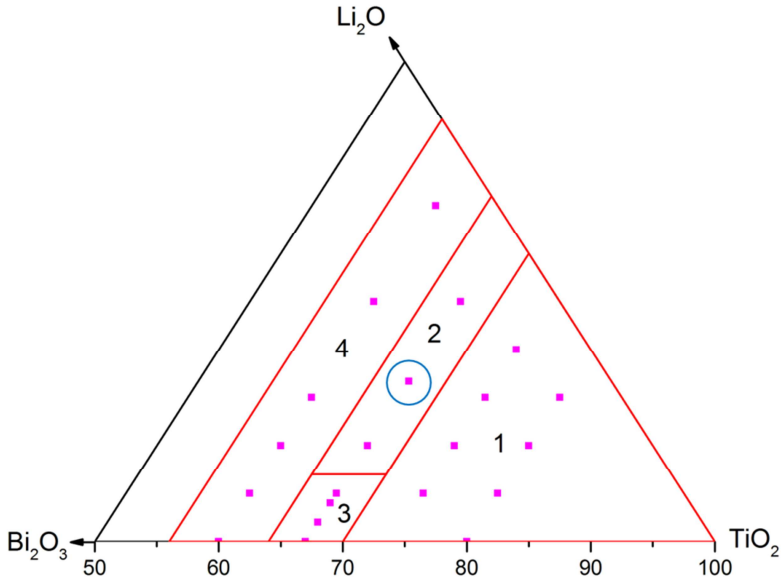

Fig. 3: Phase diagram of the ternary system TiO_2 -Bi_2O_3 - Li_2O (compositions in mol %) indicating the calcined compositions (color online)

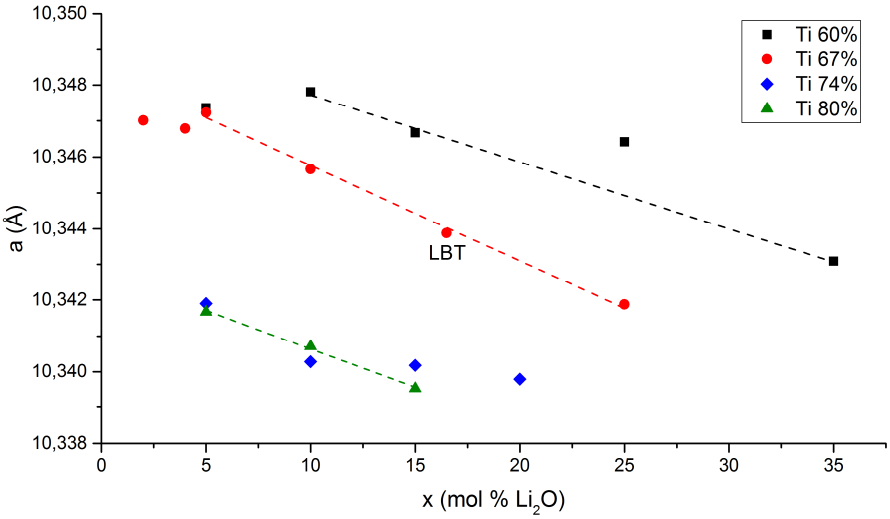

Fig. 4: Evolution of the lattice parameter of the pyrochlore phase along four diagonals of the phase diagram (color online)

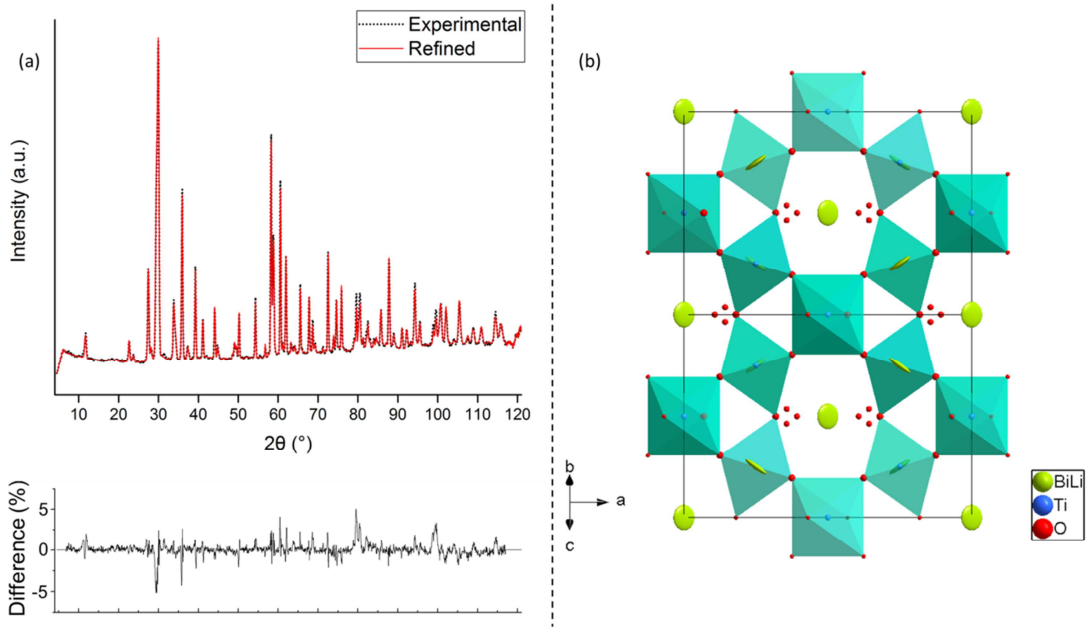

Fig. 5: (a) Final profile for the refinement of the LBT compound and (b) Representation of the pyrochlore $Li_{0.38}Bi_{1.62}Ti_2O_6O'_{0.89}$ structure in the $Fd\bar{3}m$ space group (color online)

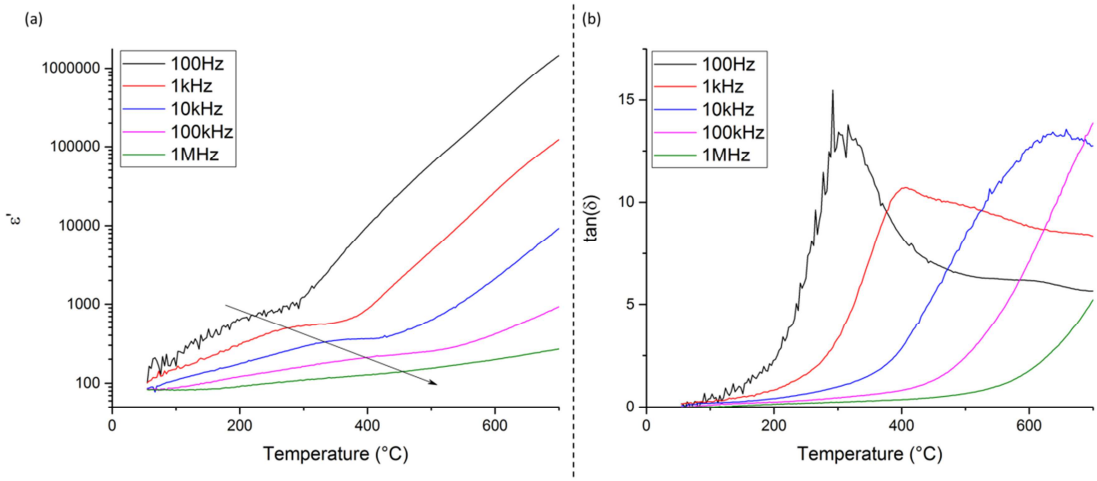

Fig. 6: (a) Relative permittivity ε' and (b) dielectric losses for the LBT ceramic sample (the arrow indicates increasing frequencies, color online)

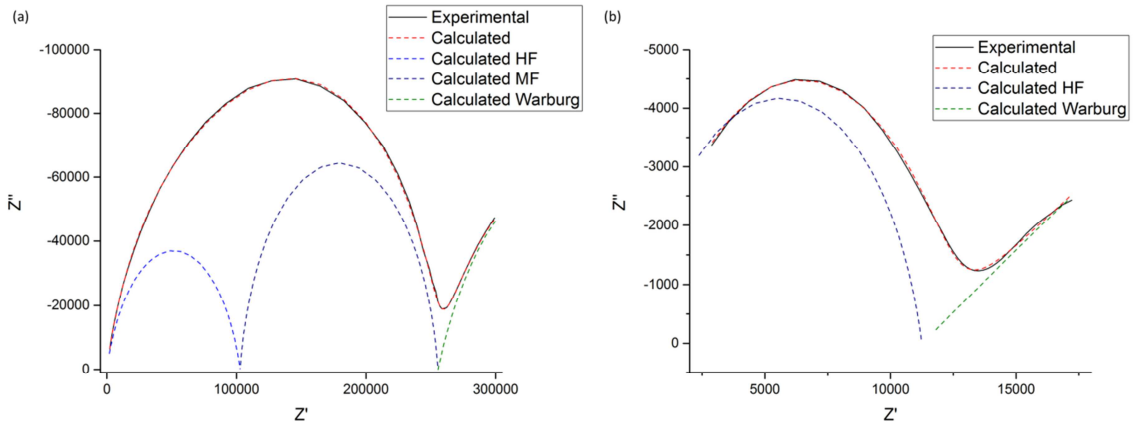

Fig. 7: Examples of two refined Nyquist diagrams: (a) at 325°C (low temperature range and (b) 550°C (high temperature range) (color online)

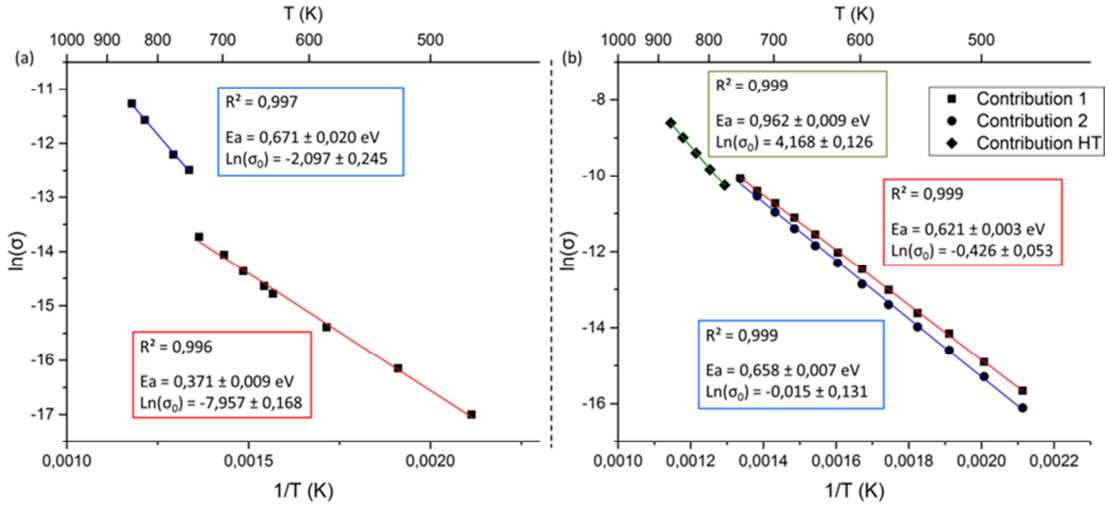

Fig. 8: Arrhenius plot of the data obtained for LBT ceramic sample from (a) DC measurements and (b) the AC impedance circles (color online)

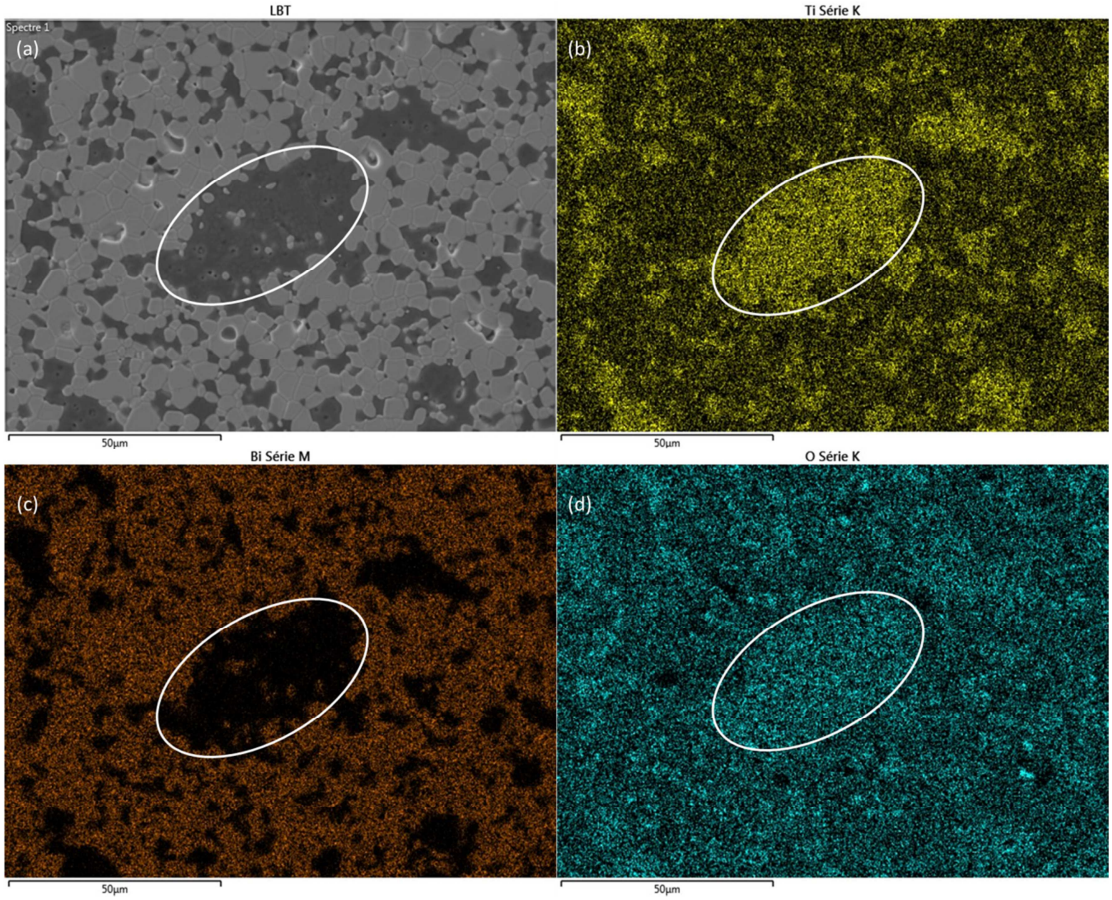

Fig. 9: (a) SEM observation of the LBT pellet and EDX study of the pellet for (b) Ti, (c) Bi and (d) oxygen (color online)

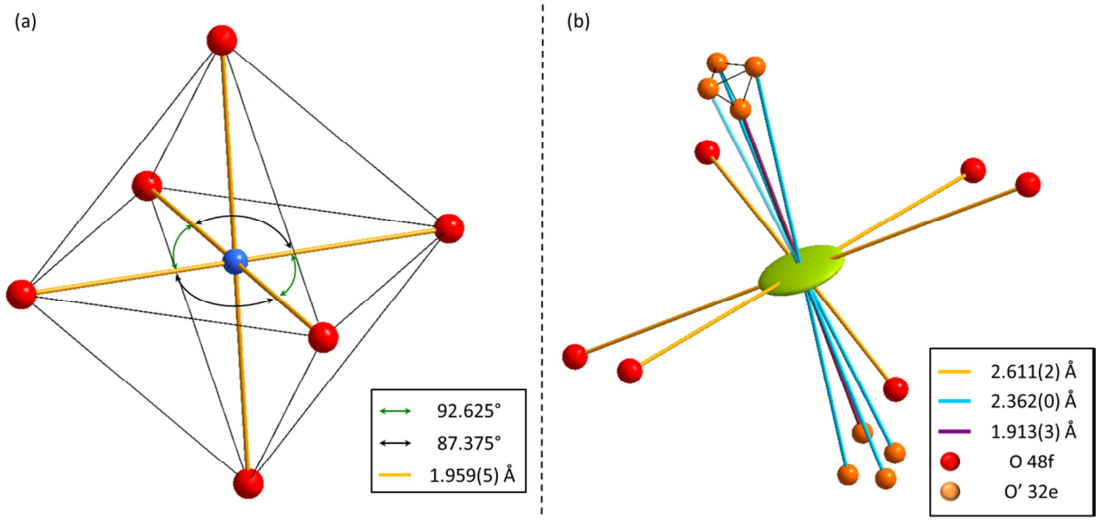

Fig. 10: cation coordination spheres with selected bond lengths and angles for (a) titanium) and (b) bismuth (color online)